Neuro-Oncology 14(1):64–78, 2012.
doi:10.1093/neuonc/nor182
Advance Access publication October 20, 2011

Microglia isolated from patients with glioma gain antitumor activities on poly (I:C) stimulation

Tim Kees, Jennifer Lohr, Johannes Noack, Rodrigo Mora, Georg Gdynia, Grischa Tödt, Aurélie Ernst, Bernhard Radlwimmer, Christine S. Falk, Christel Herold-Mende, and Anne Régnier-Vigouroux

INSERM U701, German Cancer Research Centre, INF 242 (T.K., J.N., R.M., A.R.-V.); Department of Neurosurgery (J.L., C.H.-M.) and Department of Pathology (G.G.), Heidelberg University Hospital, INF 200/221; Division of Molecular Genetic, German Cancer Research Centre, INF 580, (G.T., A.E., B.R.); and National Center for Tumor Diseases and Institute for Immunology, INF 460, Heidelberg, Germany (C.S.F.)

The role of microglia, the brain-resident macrophages, in glioma biology is still a matter of debate. Clinical observations and in vitro studies in the mouse model indicate that microglia and macrophages that infiltrate the brain tumor tissue in high numbers play a tumor-supportive role. Here, we provide evidence that human microglia isolated from brain tumors indeed support tumor cell growth, migration, and invasion. However, after stimulation with the Toll-like receptor 3 agonist poly (I:C), microglia secrete factors that exerted toxic and suppressive effects on different glioblastoma cell lines, as assessed in cytotoxicity, migration, and tumor cell spheroid invasion assays. Remarkably, these effects were tumor-specific because the microglial factors impaired neither growth nor viability of astrocytes and neurons. Culture supernatants of tumor cells inhibited the poly (I:C) induction of this microglial M1-like, oncotoxic profile. Microglia stimulation before coculture with tumor cells circumvented the tumor-mediated suppression, as demonstrated by the ability to kill and phagocytose glioma cells. Our results show, for the first time to our knowledge, that human microglia exert tumor-supporting functions that are overridden by tumor-suppressing activities gained after poly (I:C) stimulation.

Keywords: antitumor response, glioma, human microglia, poly (I:C).

Glioblastoma multiforme (GBM) belongs to the most fatal cancers. Main obstacles for effective treatments are their resistance to cell death and their high invasive phenotype. Together with blood-borne macrophages, microglia, the brain-resident macrophages, infiltrate GBM tissues extensively, contributing up to 30% of the total tumor mass.[1] Despite their cytotoxic and phagocytic functions,[2] these tumor-infiltrating microglia/macrophages (TIMs) seem to support tumor growth rather than suppress it. Patients with a higher number of TIMs have worse prognosis. Several tumor-derived factors, such as transforming growth factor (TGF)−β or interleukin (IL)−10 inhibit microglial immune functions[3] and induce these cells to adopt an M2-like, tumor-supportive and anti-inflammatory profile.[4] Macrophages become tumoricide after stimulation through their toll-like receptors (TLRs).[5,6] Located at the cell membrane and in endosomes, TLRs are activated by pathogen-associated molecular patterns, such as lipopolysaccharides (LPS) or viral RNA molecules, or by molecules released by tumor cells.[6] This activation induces a pro-inflammatory M1 profile, associated with secretion of factors, such as tumor necrosis factor (TNF)−α, interferons (IFNs), and IL-12, which can contribute to tumor growth suppression.[4] Activation via TLR3 agonists, such as polyinosinic-polycytidylic acid (poly [I:C]), seem to induce the strongest pro-inflammatory response in human microglia[7] that enables these cells to mediate a Th_1 polarization of CD4 T cells.[8] The pioneer studies of Hussain et al. on TIMs freshly isolated from human brain tumor tissues revealed an intact phagocytic function but an inactive immune profile, despite the expression of TLRs, and a low tumoricidal capacity of these cells.[9] We hypothesized that, given microglial

Received December 6, 2010; accepted September 2, 2011.

Corresponding Author: Anne Régnier-Vigouroux, DKFZ, INF 242, 69120 Heidelberg, Germany (regnier@dkfz.de).

plasticity, a proper activation of TIMs may divert them from their tumor-supporting functions and trigger their tumor-suppressing activities. Here, we show that human TIMs indeed support tumor growth and invasion. However, after treatment with the TLR3 agonist poly (I:C), they gain efficient and specific antitumor activities that comprise tumor cell death and inhibition of tumor cell growth and invasion.

Materials and Methods

Cells and Culture Media

Human primary (NCH82, 149, 210) and secondary (NCH199) glioblastoma cell lines and the NCH421k glioblastoma stem cell line were generated at the Department of Neurosurgery, Heidelberg University Hospital (Heidelberg, Germany)[10,11] and were used at low passage numbers (20–50). Non–stem cell cultures were grown in complete growth medium (cDMEM) made of Dulbeccos's Modified Eagle Medium (DMEM high glucose; Sigma), 10% heat-inactivated fetal calf serum (FCS; PAA), 2 mm glutamine (Invitrogen), and 50 μg/mL gentamycin (Invitrogen). Stem cells were grown in BIT-medium made of DMEM, 20% BIT (bovine serum albumin [BSA], insulin, transferrin; ProVitro) serum-free supplement, basic fibroblast and epidermal growth factors (20 ng/mL each; ProVitro), 100 U/mL penicillin, and 100 μg/mL streptomycin (Invitrogen). Human fetal astrocytes and neurons (ScienCell) were cultured in astrocyte or neuron growth medium (ScienCell), respectively, complemented with 2% FCS.

Isolation of TIMs

An isolation protocol was established on the basis of protocols described previously.[10,12] Brain tumor tissues (1–5 g) from patients (Supplementary material, Table S1) obtained at the Department of Neurosurgery were used 1–24 h after surgery and stored until preparation at 4°C in DMEM, 10% FCS, and 100 U/mL penicillin/100 μg/mL streptomycin (see Supplementary Material for a list of the material used and respective catalog numbers). Informed consent was obtained from each patient according to the research proposals approved by the Institutional Review Board at Heidelberg Medical Faculty. Tissues were weighed, mechanically dissociated, and washed in Hanks' Balanced Salts Solution (HBSS) (Sigma). All centrifugation steps were performed at 300 *g*, 10 min, 10°C. The pelleted material was enzymatically digested with 10 mL/g of tumor tissue of HBSS containing Liberase I Blendzyme (7 Wünsch Units/mL; Roche) and DNase (250 U/mL, Roche) for 1 h at 37°C. Digestion was stopped by addition of cDMEM. After 1 wash with HBSS (optional), the cell suspension was filtered sequentially with a 100 μm then with a 40 μm cell strainer (BD Falcon) and centrifuged. The pelleted cells were resuspended and incubated in erythrocyte lysis buffer (NH_4Cl 0.15 M, $KHCO_3$ 10 mM, EDTA 0.1 mM [pH, 7.2]) for 10 min on ice. Lysis was stopped by addition of cDMEM or HBSS and centrifugation. Cells were resuspended in BIT medium and seeded on 6 cm bacterial grade dishes (Sarstedt) at 37°C, 5% CO_2, to enable TIMs to adhere while tumor cells and other types of cells remained in suspension. This adhesion step was performed for 2 h and could be extended for up to 12 h. At the end of the adhesion step, supernatants that contained mainly tumor cells were removed and either discarded or centrifuged to harvest primary tumor cells that were kept in culture in cDMEM. Adherent TIMs were washed 3 times with cDMEM and incubated in cDMEM supplemented with granulocyte macrophage colony-stimulating factor (GM-CSF; 50 U/mL; ProVitro). The whole isolation procedure took up to 3 h. TIMs were cultured in the presence of GM-CSF for 1 week and subsequently cultured in cDMEM for 1–2 weeks. This procedure yielded $\sim 4 \times 10^5$ TIMs per 6 cm dish. Successful isolation and generation of viable TIMs was achieved for ~70% of the tumor tissues. The material from each preparation (cells and supernatant) was used once in various assays.

Generation of TIMs Supernatants

TIMs were treated with poly (I:C) (25 μg/mL; InVivogen) in serum-free medium for 48 h. Culture supernatants were used immediately or frozen at −20°C. Before their application to cells, supernatants were treated with 0.05 μg/μL RNase A (Roche) at 37°C for 1 h to neutralize remnant poly (I:C). TIM supernatants and serum-free medium (control) were complemented with FCS (heat-inactivated, 10% v/v final) before their application to tumor cells or with FCS (heat-inactivated, 2% v/v final) and astrocyte or neuron growth supplement (1:100, ScienCell) before their application to astrocytes or neurons, respectively.

Labeling of TIMs for Microglia/Macrophage Markers

Flow Cytometry Analysis.—TIMs were harvested with EDTA (5 mm) in PBS (PBS-EDTA), washed in PBS, and blocked for 30 min by incubation in 10% normal goat serum (for CD11b labeling) or 10% normal mouse serum (for CD11c and CD45 labeling) in PBS. Incubation with primary antibodies was performed on ice for 30 min in the dark. Cells were washed twice in cold PBS and, when necessary, further incubated with a secondary antibody for 30 min on ice in the dark. After washes in cold PBS, cells were filtered through nylon gauze before being analyzed with a FACSCalibur flow cytometer (BD Biosciences).

The following antibodies were used: CD11b (IgG1 mouse anti-human, BD Biosciences), CD11c-FITC and CD45-APC (IgG1 mouse anti-human; Immunotools); and goat anti-mouse PE conjugated antibody (BD Biosciences). The appropriate isotype control (mouse IgG1; Immunotools) was used for each labeling.

Immunofluorescence Analysis.—TIMs cultured in 6 cm dishes were incubated at 37°C with acetylated low density lipoprotein (AcLDL; a scavenger receptor ligand) coupled to Alexa 488 (2 μg/mL; Invitrogen). After 30 min of incubation, cells were monitored by microscopy.

Cytospin Analysis.—Cells in suspension or adherent cells harvested with PBS-EDTA were washed twice with PBS; 4×10^4 cells were centrifuged in 200 μL PBS in a cytospin cup on a glass slide. Slides were dried at 37°C for 24 h, fixed in −20°C cold acetone for 10 min, and stored at −80°C. The first antibody (CD68; BMA Biomedicals) was applied in antibody-diluent (DAKO) for 1 h at room temperature. After 3 washes in PBS, incubation with the secondary antibody (biotinylated sheep anti-mouse; Sigma) and detection were performed, as described elsewhere,[13] using the Vectastain Laboratories Elite ABC Kit (Vector Laboratories).

Cytokine Measurement

Assays were performed in triplicate with material from 3 different patients who received a diagnosis of grade IV GBM. TIMs and primary tumor cells from the same patient were isolated as described above. TIMs (10^5 cells/well) and tumor cells (10^5 cells/well) were seeded in 12-well plates either alone or together. One day after seeding, cells were left untreated or treated with poly (I:C) (25 μg/mL). A set of TIMs was treated with poly (I:C) in the presence of supernatants of confluent primary tumor cells cultures. Following incubation for 48 h, supernatants were harvested, centrifuged, and kept frozen. IL-10 and TNF-α secretion was measured using IL-10 ELISA set (Immunotools) and OptEIA human TNF ELISA set (BD) according to the manufacturers' instructions. IL-1Ra and IL-12 (p40) were measured with the BioPlex Cytokine Assay (BioRad), according to the manufacturer's instructions.

FACSArray Cytotoxicity Assay

Assays were performed in duplicate with the supernatants of different TIM preparations, as previously described.[14] In brief, cells seeded in 96-well plates (per well: 3000 tumor cells, 5000 astrocytes, 10 000 neurons) were treated 24 h later with TIM supernatants for 96 h in the absence or presence of 3-methyladenine (3-MA, 1 mm; SIGMA) or of the pan-caspase inhibitor Z-VAD-fmk (dissolved in DMSO, 20 μM; Calbiochem). At the end of the treatment, cells were incubated for 1 h with 2.5 μg/mL of acridine orange (AO; Sigma). Supernatants and cells were harvested, centrifuged in V-shaped 96-well plates, and resuspended in FACS Sheath Solution with Surfactant (BD Biosciences). Analysis was performed at the FACSArray bioanalyzer (BD Biosciences) at the yellow parameter (532 nm excitation, 564–606 nm emission) to detect positive AO staining. AO staining depends on the presence of intact acidic vesicles in living cells. Dead cells were therefore distinguished by their lack of AO labeling. They were quantified as AO-negative cells using the FACSArray internal analysis software and expressed as a percentage of total cells in each well. Living treated cells were expressed as a percentage of living control (untreated) cells.

Wound Healing Assay

Monolayer wound healing assays were performed as described elsewhere.[15] Cells were grown to 90% confluence in 12-well plates. Growth medium was then exchanged for PBS, and cell monolayers were wounded with a plastic tip (1 mm), washed twice with PBS, and incubated in different conditions. Migration was monitored by photographing cells with an inverted Leica DFC 350 FX phase contrast microscope coupled to a Leica Firecam system (Leica, Germany) at 4× (NCH82 cells) or 10× (NCH210 cells) magnification at the indicated times.

Spheroid Culture and Invasion Assay

Invasion assays were performed as described elsewhere,[14] with use of spheroids with a diameter of ∼800 μm. Spheroids were generated from 25 μL drops of cell suspensions (NCH82, 10^6 cell/mL; NCH210, 1.5×10^6 cell/mL; mixed spheroids: TIMs 5×10^5 cell/mL, NCH82 5×10^5 cell/mL). Photographic documentation of migration was performed as described for the wound healing assay. Measurement and calculation of invaded areas were done with the Zeiss Axio Vision Release 4.6.3-SP1 software. The area covered by the initial spheroid at $t = 0$ was subtracted from the area covered by the spheroid and migrating cells at various times of treatment. Means ± standard error of the mean of invaded areas were calculated and expressed as percentage of the area invaded in control conditions for each time.

Cocultures of Tumor Cells and TIMs

Cocultures in Collagen Matrix.—Tumor cells (before spheroid generation) and TIMs (after 48 h treatment with or without 25 μg/mL poly [I:C]) were labeled with the lipophilic fluorescent dyes DiI and DiO, respectively, as follows. TIMs (extensively washed to remove any remnant poly [I:C]) and glioma cells (10^6/mL) were resuspended in serum-free medium and incubated with the dyes (2.5 μM; Invitrogen) for 15 min. Following washes in growth medium, the TIMs were resuspended in liquid collagen (2.5×10^5 cells/250 μL) and distributed in 8-well LabTek chambers. Labeled tumor cell spheroids were then added to the wells. After solidification, matrices were overlaid with 150 μL cDMEM. Cells were incubated for 2 weeks in cDMEM (devoid of poly [I:C]), with medium changes every 5 days. Eventually, they were labeled with TO-PRO-3 (1 μM; Invitrogen) for at least 5 h before confocal microscopy (Leica TCS SP5). Optical slices were acquired in 1.5 μm steps to a total depth of ∼300 μm per stack.

Scanning was performed in a sequential mode with a 10×/0.7 dry objective lens with the following parameters: DiO (excitation: argon-laser 488 nm; emission: 498–553 nm), DiI (excitation: argon-laser 543 nm; emission: 553–643 nm), TO-PRO-3 (excitation: helium/neon-laser 633 nm; emission: 643–720 nm). AmiraVis Amira (Visage Imaging) software was used for the 3D modelling of captured stacks.

Two-photon microscopy was performed on an Olympus FluoView 1000 MPE with an infrared (IR) corrected 20×/1.2 objective lens with an excitation of 950 nm and a detection range of 495–540 nm (DiO) and 575–630 nm (DiI).

Cocultures in Monolayers.—Growth medium of TIMs cultured in 6 cm Petri dishes (~4×10^5 cells per dish) was exchanged for serum-free medium or serum-free medium containing poly (I:C) (25 μg/mL). After 2 days of incubation, supernatants were removed, TIMs washed 3 times with cDMEM, and 5×10^5 NCH82 cells labeled with carboxyfluorescein diacetate succinimidyl ester (CFSE; 5 μM, 15 min, 37°C) were added per dish. Cells were co-incubated for 4 days and photographed with an inverted Leica DFC 350 FX phase contrast microscope coupled to a Leica Firecam system.

Phagocytosis Assay

The assay was performed essentially as described elsewhere.[16] At day 0, TIMs (3×10^5 cells/well) and NCH82 cells (10^6 cells/dish) were seeded in cDMEM on 6-well plates and on 10 cm dishes, respectively. At day 1, growth medium of TIMs was exchanged for serum-free medium, and cells were either stimulated with 25 μg/mL poly (I:C) or left unstimulated for 48 h. At day 2, NCH82 cells were intoxicated by addition of 500 μg/mL etoposide in cDMEM and incubated over night. At day 3, adherent NCH82 cells were detached with PBS-EDTA, pooled with floating apoptotic cells, washed, and resuspended at 10^6 cells/mL in serum-free DMEM. NCH82 cells were then labeled with CFSE, washed 3 times in cDMEM, and 3×10^5 cells added to wells containing TIMs. After 1 h of co-incubation, cells were washed, detached with PBS-EDTA, labeled for CD11b as described above, and analyzed at the FACSCalibur flow cytometer. TIMs (CD11b positive, red fluorescence) that had engulfed tumor cells (CFSE labeling, green fluorescence) were identified as double positive cells.

Transcriptional Profile Analysis

The transcriptional profile was evaluated in 5 independent TIM preparations (grades II to IV) either left untreated or treated with poly (I:C) 25 μg/mL for 48 h. Total cellular RNA was isolated using the miRNeasy Mini kit (Qiagen). Global gene expression profiling was conducted using Agilent Whole Human Genome 4 × 44 K Oligo Microarrays (Agilent Technologies) according to the manufacturer's recommendations. Microarray read-out was obtained using an Agilent Scanner G25505B with automatically adjusted PMT voltages. Raw intensity tables of recorded images were generated using Feature Extraction 9.1 software and processed on the in-house-developed ChipYard analysis platform (http://www.dkfz.de/ChipYard/).

Statistical Analysis

Statistical significance was determined using the Student's t test ($P < .05$). Data are expressed as mean ± standard error of the mean. The asterisks represent values significantly different from the control group (medium, or treated cells in the absence of inhibitors); $*P < .05$; $**P < .01$; $***P < .005$.

Results

Phenotypic Characterization of TIMs

We first optimized the TIM isolation procedure to obtain sufficient amounts of cells. Percoll gradients are usually performed to separate TIMs from tumor cells. Although it is convenient for ex vivo analysis,[9] this procedure is not ideal if isolated cells are to be kept in culture,[17] namely because of an impaired viability (personal observations). To circumvent this problem, we established another protocol based on the capability of microglia and macrophages to adhere quickly and firmly to bacterial-grade Petri dishes. Another important modification was the use of BIT medium, which promoted TIM adhesion while diminishing that of tumor cells and, thus, strongly increased yields of TIMs. The isolation procedure comprised mechanical dissociation, enzymatic digestion, and incubation in BIT medium on Petri dishes for 2 h (Fig. 1A). During this time, TIMs attached to the plate surface while other cells stayed in suspension. After this isolation step, adherent cells were found to be positively stained for the phagocyte marker CD68, whereas nonadherent cells were negative (Fig. 1B). Following cultivation for 7 days in the presence of GM-CSF, adherent cells showed typical microglial morphology (fusiform and amoeboid cells with hair-like pseudopodia) (Fig. 1B). More than 90% of these cells took up AcLDL, as shown by microscopy (Fig. 1B) and flow cytometry analysis (not shown), indicating expression of a functional scavenger receptor. They were positive for the leukocyte common antigen CD45 and the microglia/macrophage markers CD11b, CD11c (Fig. 1B and C), and Iba1 (not shown). Furthermore, they were able to engulf etoposide-treated dead glioma cells (Fig. 1D and E). All together, these data demonstrate that the modified procedure led to the successful isolation of functional TIMs.

TIMs Acquire Tumor-Suppressing Activities after Treatment with Poly (I:C)

Poly (I:C) was the only TLR agonist that triggered an antiproliferative activity of TIMs toward the NCH82

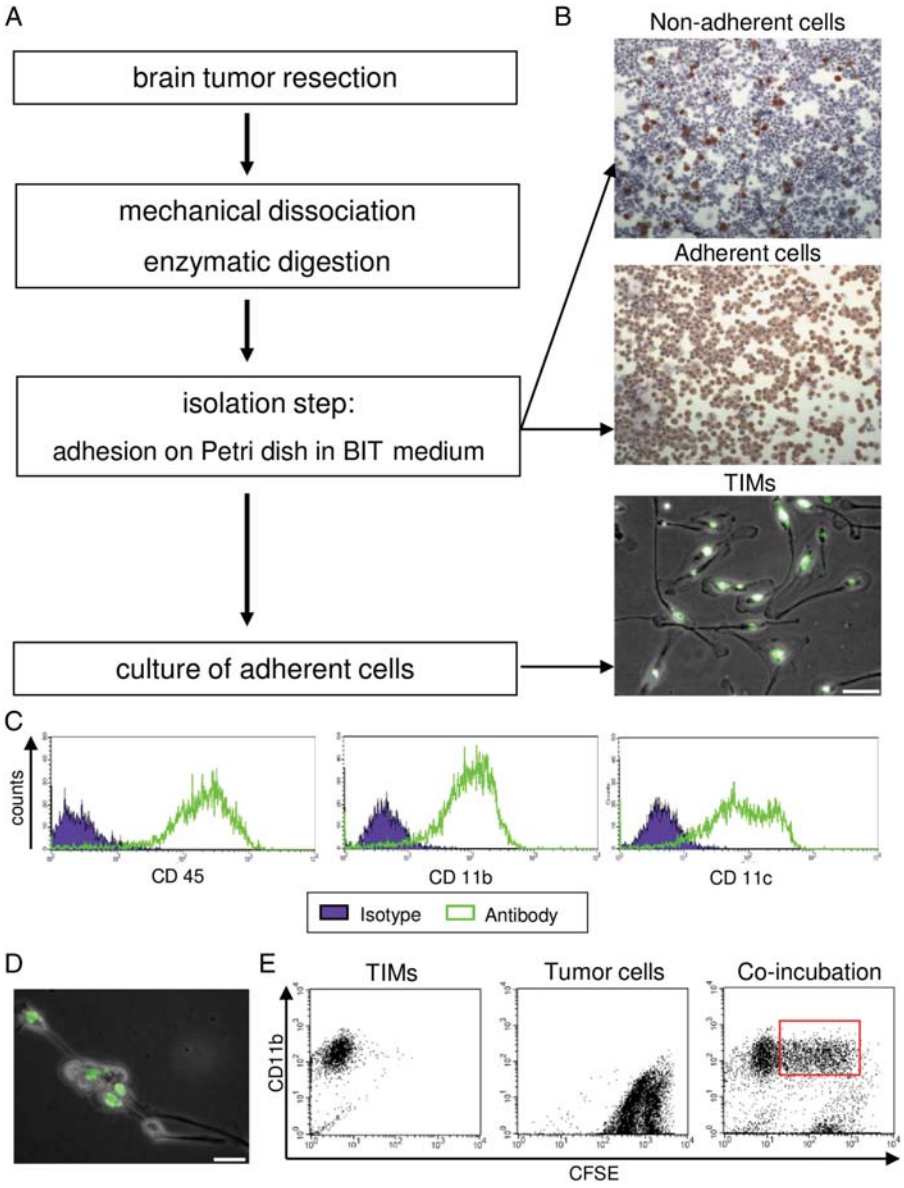

Fig. 1. Isolation and characterization of human tumor-infiltrating microglia. (A) Isolation procedure. (B) Cytospin preparations of nonadherent cells *(top)* and adherent cells *(middle)* were labeled for CD68. Isolated TIMs take up fluorescent AcLDL (*bottom*; bar = 100 μm). (C) Flow cytometry analysis of isolated TIMs. (D, E) TIMs phagocytose etoposide-treated CFSE-labeled NCH82 cells. (D) confocal microscopy (bar = 50 μm). (E) Flow cytometry: CD11b-labeled TIMs *(left)* and CFSE-labeled, etoposide-treated NCH82 cells *(middle)* were coincubated for 2 h (right). Red box: double-positive cells indicate TIMs that engulfed glioma cells. Data from one representative TIM preparation ($n = 5$).

glioma cells (Supplementary material, Fig. S1A). Direct application of the agonist on glioma cells only slightly affected their proliferation (Supplementary material, Fig. S1A). Pretreatment of TIM supernatants with RNase ruled out a direct toxic effect of poly (I:C) on tumor cells (data not shown). This lack of direct toxicity was further confirmed by the viability and migration capacity of NCH82 cells in spheroids treated with poly (I:C) for up to 5 days (see Fig. 6A). Unsupervised cluster analysis of whole transcriptome data indicated a clear classification of untreated and treated TIMs in 2 distinct groups, strongly suggesting the absence of gross individual variability among TIM preparations (Fig. 2A). In addition to the expected morphological change (Supplementary material, Fig. S1B), poly (I:C) treatment polarized TIMs toward an M1-like profile, as indicated by their secretion of high TNF-α and IL-12 amounts (Supplementary material, Table S2) and by their transcriptome expression (Fig. 2B, Supplementary material, Table S3).

Cytotoxic and antiproliferative activities of TIM preparations ($n > 20$; 4 representative preparations shown) were assessed on 4 glioma cell lines. Treatment with supernatants of poly (I:C)–stimulated TIMs

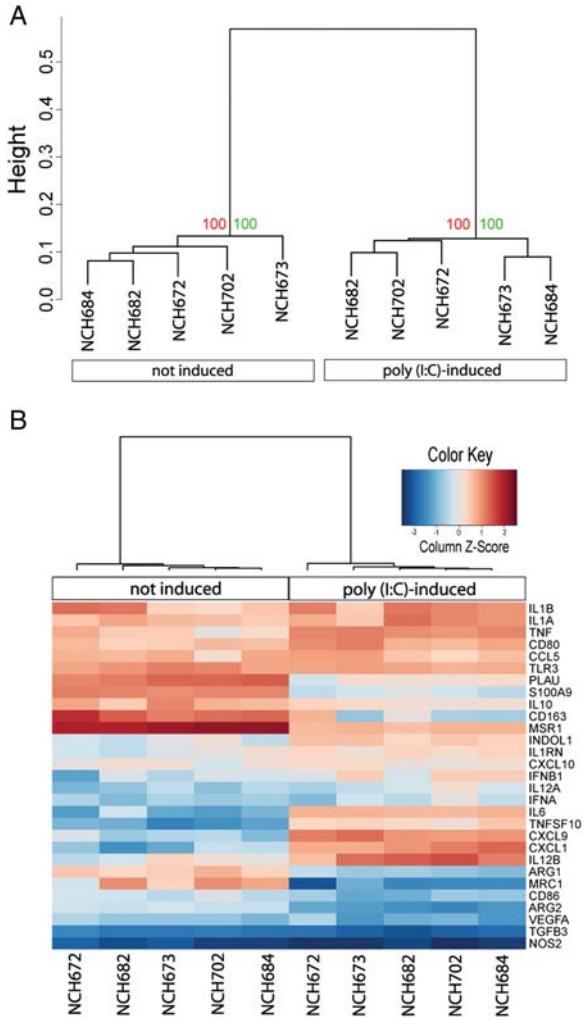

Fig. 2. Poly (I:C)–activated TIMs express an M1-like profile. Unsupervised hierarchical cluster analysis of unstimulated and poly (I:C)–stimulated (48 h) TIM samples based on (A) whole-transcriptome analysis and (B) the expression of 29 M1-M2 related genes (see Supplementary material, Table S3) shows clear separation of stimulated and unstimulated samples. Numbers at the base of clusters indicate bootstrap support. Heatmap (B) reflects the gene expression ratios of the M1-M2 classifier genes.

(SN+) led to a high (50%–90% dead cells; NCH82, NCH149), intermediate (~40% dead cells; NCH199) and low (<20% dead cells; NCH210) rate of glioma cell death (Fig. 3A). The decreased number of living NCH199 and NCH210 cells indicated a strong antiproliferative activity for these supernatants, which did not affect astrocyte (Fig. 3A) or neuron (Fig. 3B) survival.

Treatment with supernatants of unstimulated TIMs (SN) did not affect the number of living cells; it even increased that of some NCH cells and astrocytes. Antiproliferative effects (see NCH210 cells) or cytotoxicity (<20% dead cells) (Fig. 3A and B) were rarely observed, indicating that tumor-specific toxic effects resulted from TIM activation. Trypsin or heat pretreatment of SN+ abolished its cytotoxicity, demonstrating the proteinaceous nature of factors released by TIMs after poly (I:C) stimulation (Supplementary material, Fig. S1C). These factors triggered apoptosis of the glioma cells as shown in Fig. 3C. Indeed addition of the pan-caspase inhibitor Z-VAD strongly reduced SN+-induced cell death, whereas addition of 3-MA, an inhibitor of autophagosome formation,[18] did not protect the glioma cells from death.

Stimulated TIMs Secrete Factors that Decrease Glioma Cell Invasion and Migration

In agreement with the hierarchical clustering of genes reported in Fig. 2A, the various TIM preparations exhibited a rather homogenous profile of activity toward glioma and primary brain cells. Variations in the extent of the effects mainly depended on the glioma cell lines. Two cell lines, showing sensitivity (NCH82) or resistance (NCH210) to SN+ toxicity, were chosen for further characterization of TIMs' antitumor activities. Treatment of NCH82 spheroids with SN+ led to decreased invasiveness (Fig. 4A) and to death, as indicated by the rounded-up morphology of cells present in the invaded area (Fig. 4A, magnified insert). Treatment with SN slightly, but significantly, increased invasion of cells that showed an elongated morphology (Fig. 4A) similar to that observed in control conditions (not shown). NCH210 spheroids treated with SN+ also exhibited decreased invasiveness (Fig. 4B) but no morphological evidence for death (Fig. 4B, magnified insert), consistent with their resistant phenotype. Invasion ability of NCH210 spheroids was not affected by SN. The different effects exerted by TIM SN on NCH82 and NCH210 spheroid invasion suggested that different matrix MMP activities may be displayed by the glioma cells and/or by the various TIM preparations. This, however, was not the case, as indicated by zymography analysis. The 4 glioma cell lines used in this study showed the same profile of MMP9 low and MMP2 high activities. Of interest, every TIM preparation tested exhibited a profile complementary to that of the glioma cells (MMP9 high and MMP2 low). This profile did not change after their stimulation with poly (I:C) (Supplementary material, Fig. S2A). Spheroids of glioma stem cells treated with TIM supernatants exhibited an invasion profile comparable to that of NCH210 (Supplementary material, Fig. S2B).

Cytotoxic and antimigratory activities both contribute to changes in invasiveness. These activities were monitored in wound healing assays that provided a measure of cell migration and facilitated cell death assessment. Migration profiles of NCH82 (Fig. 5A) and NCH210 (Fig. 5B and C) cells in any treatment condition were very similar to that observed in collagen invasion assays. We analyzed NCH82 and NCH210 cells at different time points because they differed in the size of the gap created after scratching. Morphological analysis confirmed the presence of migrating (elongated) NCH82 and NCH210 cells at the migration front of glioma

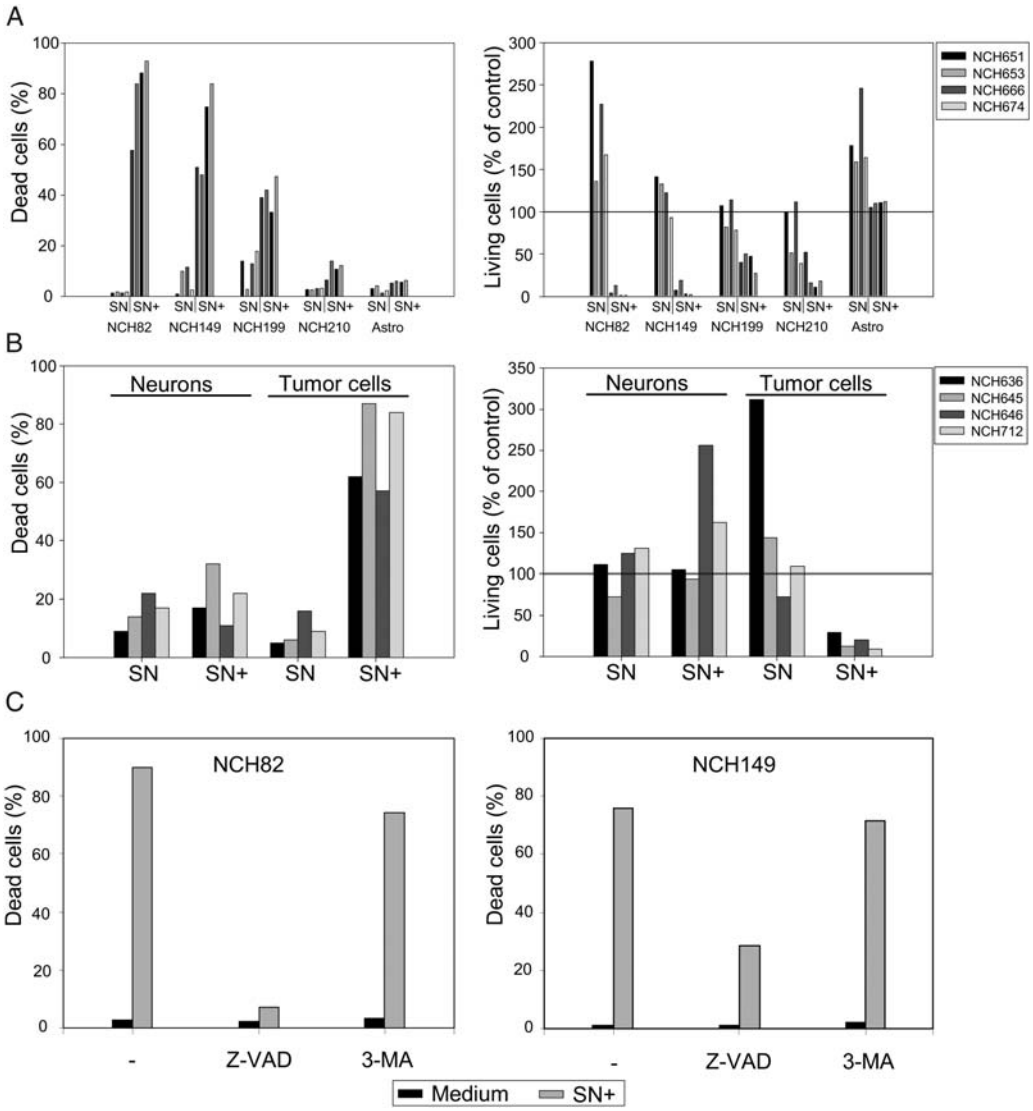

Fig. 3. TIM factors affect tumor cells viability. (A) Effect of supernatants of unstimulated (SN) and poly (I:C)–stimulated (SN+) TIMs on glioma (NCH) cells and astrocytes (Astro) viability and death. (B) Effect of TIM supernatants on NCH149 cells and neuron viability and death. Boxes to the right: identification number of patients from whom TIMs were derived. (C) SN+ induces apoptotic cell death in glioma cells. NCH82 and NCH149 glioma cells were incubated in medium *(black bar)* or treated with SN+ *(gray bar)* in the absence (-) or presence of Z-VAD (20 μM) or 3-MA (1 mm) for 4 days. SN+ gained from TIMs derived from NCH628 and NCH645 tissue samples were used with NCH82 and NCH149 cells, respectively. A representative experiment is shown (NCH82, $n = 3$; NCH149, $n = 2$).

cells kept in medium or treated with SN. NCH82 cells treated with SN+ displayed a rounded up morphology at the migration front and a disorganised cell layer, suggesting ongoing cell death. Contrary to control and SN-treated NCH210 cells, SN+-treated NCH210 cells showed a smooth migration front and a dense cell layer, suggesting active cell proliferation without migration (Fig. 5C). Flow cytometry analysis (Supplementary material, Fig. S3A and B) indicated an increased number of dead NCH82 cells after SN+ treatment (dead cells in medium: 38%; in SN: 40%; in SN+: 78%) that was not observed for NCH210 cells (dead cells in medium: 12%; in SN: 8%; in SN+: 15%). This demonstrates that factors secreted by stimulated TIMs exert true antimigratory effects.

Glioma Cells Impair TIMs Poly (I:C) Stimulation

We next investigated whether TIM antitumor properties could be activated by poly (I:C) in the presence of glioma cells. For that purpose, we monitored tumor cell invasion from mixed tumor cell-TIM spheroids after poly (I:C) stimulation. After 24 h of treatment, cell migration was detectable in all but one condition: that of poly (I:C)-treated NCH82-TIM spheroids. This lack of

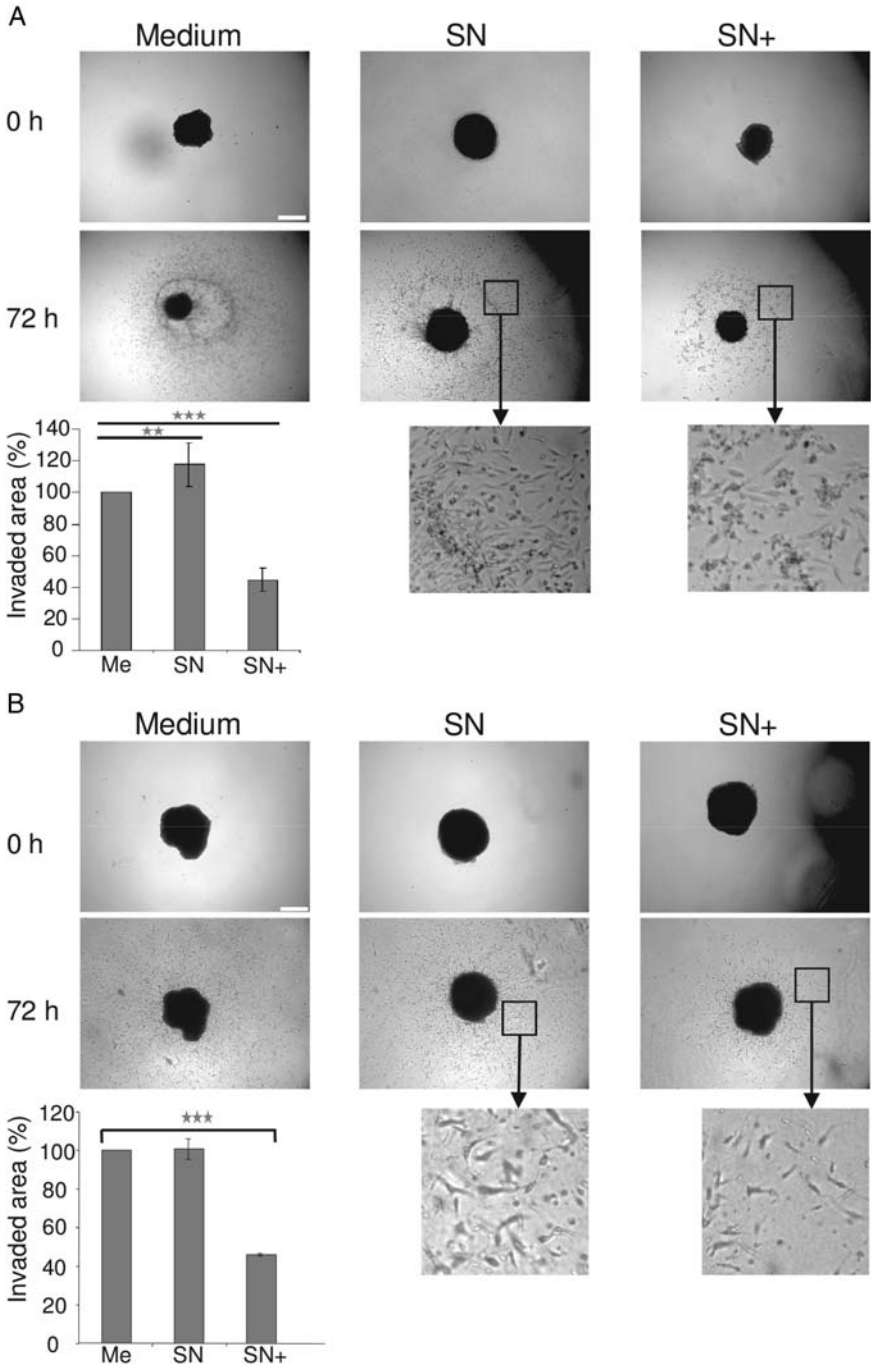

Fig. 4. TIM factors affect tumor cell invasion. NCH82 (A; $n = 5$) or NCH210 (B; $n = 3$) spheroids were treated with medium or supernatant of unstimulated (SN) or stimulated (SN+) TIMs. Pictures were taken at 0 h and 72 h of treatment. Bar = 400 μm. Magnification (40×) boxes: cell morphology at 72 h of treatment. Data from one representative TIM preparation. Graphs: quantification of area invaded by cells at 72 h. Data are expressed as mean ± SEM of invaded areas relative to medium condition.

migration was accompanied by the presence of cell-free areas within the spheroids. This inhibitory effect was no longer observed at 144 h, as indicated by similarities in invasion areas, irrespective of treatment conditions or spheroids composition (Fig. 6A), suggesting a deficient stimulation of the numerous TIMs (Fig. 6B) in the presence of glioma cells. Analysis of primary glioma cells and TIMs derived from the same tumor tissue showed that IL-12 and TNF-α production by poly (I:C)–treated TIMs was drastically decreased in presence of glioma supernatants (Fig. 6C). Moreover poly (I:C) treatment of primary glioma cells increased their production of IL-1 receptor agonist (IL-1Ra) and IL-10, thereby possibly enhancing their anti-inflammatory activity.

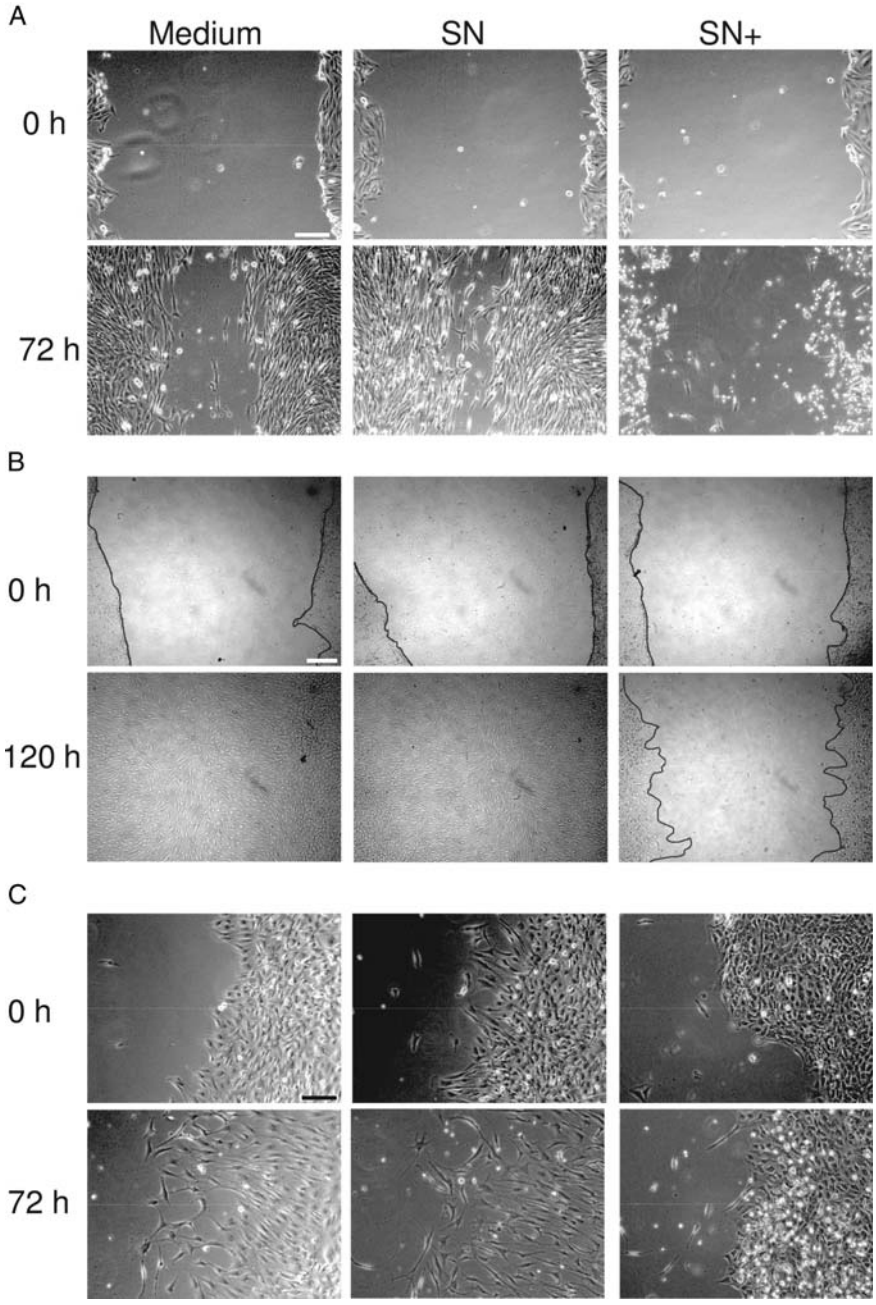

Fig. 5. TIM factors affect tumor cell migration. Wound healing assays were performed with NCH82 (A; bar = 200 μm) and NCH210 (B, bar = 400 μm; C, bar = 200 μm) cells treated with medium or supernatant of unstimulated (SN) or stimulated (SN+) TIMs. Black lines in B: migration front. Data from one representative TIM preparation ($n = 4$).

Prestimulated TIMs Kill and Phagocytose Glioma Cells

Because of the failure of poly (I:C) to stimulate TIMs present in a tumor mass, we addressed the possibility of using exogenously prestimulated TIMs to kill glioma cells in the tumor tissue. We first assessed whether poly (I:C)–stimulated TIMs keep their toxic activities after withdrawal of the stimulus. In these experiments, CFSE-labeled NCH82 cells were added to TIMs after thorough washes of the poly (I:C) stimulus. Unstimulated TIMs supported growth and survival of glioma cells (Fig. 7A). Pre-poly (I:C)–stimulated TIMs further cultured in absence of poly (I:C) with glioma cells for 4 days induced tumor cell death, as indicated by morphology (Fig. 7A, right panel) and flow cytometry analyses (data not shown), and they phagocytosed dying NCH82 cells (Fig. 8A). TIMs, therefore, keep their poly (I:C)–induced tumoricidal properties after stimulus withdrawal.

Using a collagen coculture model, we next investigated the antitumor activities of unstimulated and prestimulated TIMs on spheroids of NCH82 cells.

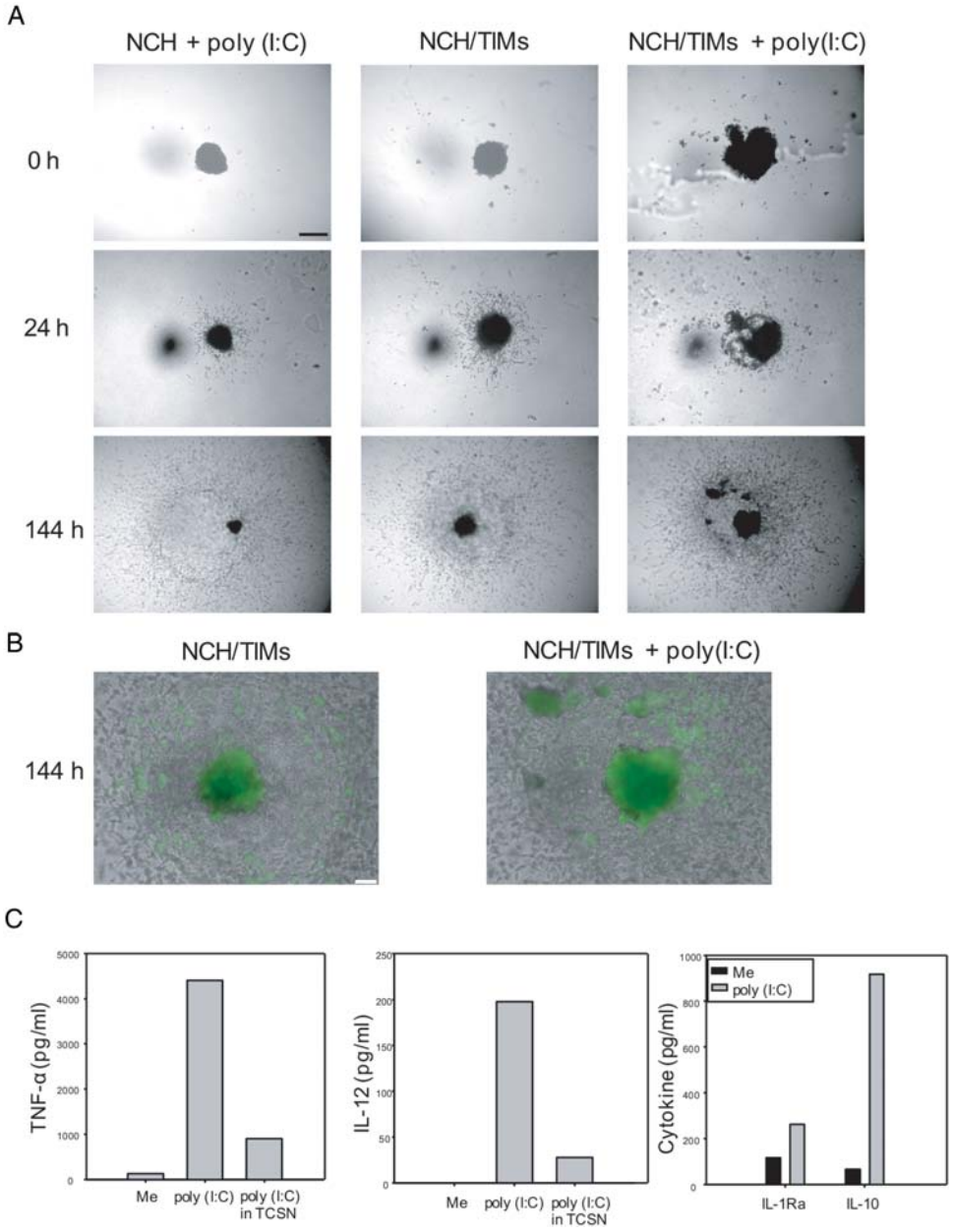

Fig. 6. Poly (I:C) treatment of mixed spheroids does not affect cell invasion capacity. (A) Spheroids of NCH82 (NCH) and mixed NCH82 cells/TIMs (NCH/TIMs) were left untreated or treated with 25 μL/mL poly (I:C) and photographed at the indicated time points. Bar = 400 μm. (B) Mixed spheroids described in (A) were labeled at 144 h with fluorescent AcLDL for 30 min before microscopic analysis in order to identify TIMs. Bar = 200 μm. Data from one representative TIM preparation ($n = 3$). (C) Cytokine response of TIMs and tumor cells upon 48 h poly (I:C) treatment. Cells were left untreated (Me) or were treated with poly (I:C) in absence or presence of primary tumor cell supernatant (TCSN; for TIMs only). Data (triplicates) from one representative cell preparation ($n = 3$).

Spheroids and their surrounding were monitored for invasion, death, and phagocytosis of glioma cells by live confocal microscopy performed over a total range of 250–300 μm. After 2 weeks in culture, spheroids implanted in a collagen matrix devoid of TIMs exhibited a core filled with dead cells (depicted in red) surrounded by a dense crown of living glioma cells (depicted in green) and by an invasion area of lower cellular density populated mainly by living cells (Fig. 7B). The presence of unstimulated TIMs did not induce drastic changes. TIMs were observed close to the spheroid and often formed clusters surrounding red dead cells (Fig. 7B). The presence of prestimulated TIMs led to a strong increase in red dead cells within the spheroid and in the invasion area and to a reduction of the spheroid (Fig. 7B). Visualization of confocal images using maximum intensity projection confirmed that dead cells were glioma cells (Fig. 7C) and

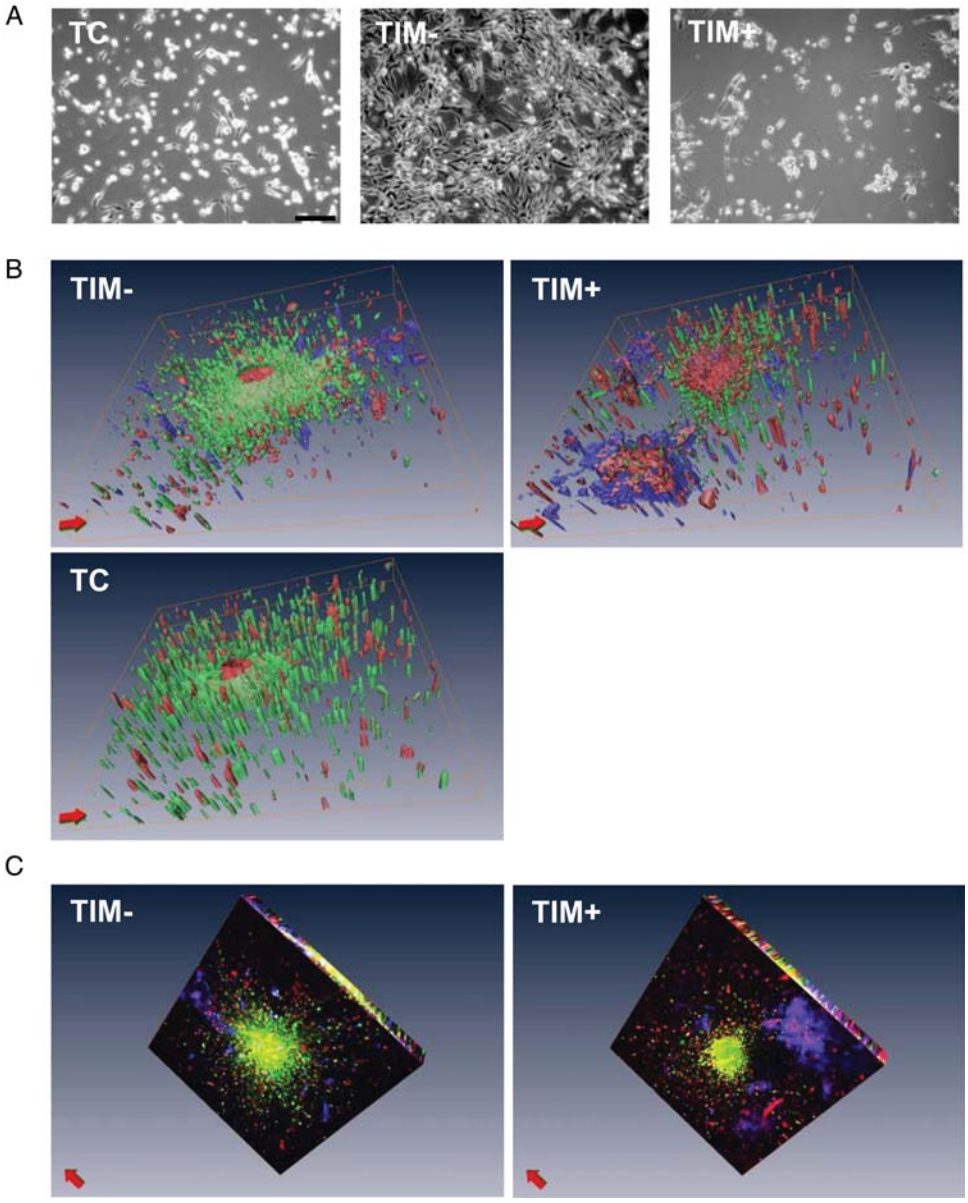

Fig. 7. TIMs pretreated with poly (I:C) kill glioma cells. (A) TIM cytotoxic activity is kept after poly (I:C) withdrawal. TIMs untreated (TIM-) or treated 48 h with poly (I:C) (TIM+) were cocultured with CFSE-labeled NCH82 cells for 4 days. TC: control culture of NCH82 cells in cDMEM. Data from one representative TIM preparation ($n = 8$). Bar = 200 μm. (B, C) Pretreated TIMs kill tumor cells in spheroid culture. TIM- and TIM+ (see legend in A) labeled with DiO were cocultured in collagen matrix with DiI-labeled NCH82 spheroids for 2 weeks. Control NCH82 spheroids (TC) were grown in the absence of TIMs. Dead cells were stained by TO-PRO-3 added 5 h before confocal microscopy. Modeling of confocal images with the Amira software was used to reconstruct 3D views of TIMs (blue label), tumor cells (green label) and TO-PRO-3 positive dead cells (red label). 3D iso-surface rendering view (B): visualization of individual populations. Maximum intensity projection (C): visualization of merged labelings. Data from one representative TIM preparation ($n = 3$).

confirmed the reduction in size (Fig. 7C). Larger clusters of TIMs surrounding dead cells were also observed. A closer analysis of these clusters using transparent projection indicated engulfment of dead (likely glioma) cells by TIMs (Fig. 8A). The apparent cell tubular morphology is attributable to modelling reconstruction. Two-photon microscopy was performed to analyze the core of the spheroids. Very few, if any, TIMs were detected in the spheroid (red glioma cells) (Fig. 8B) unless they were prestimulated (Fig. 8B). Besides clusters of green cells, numerous double-labeled areas (yellow color) were observed, suggesting ongoing phagocytic activity within the spheroid. These results demonstrate that poly (I:C) prestimulation of TIMs overcomes glioma-mediated inhibition of TIM antitumor potential.

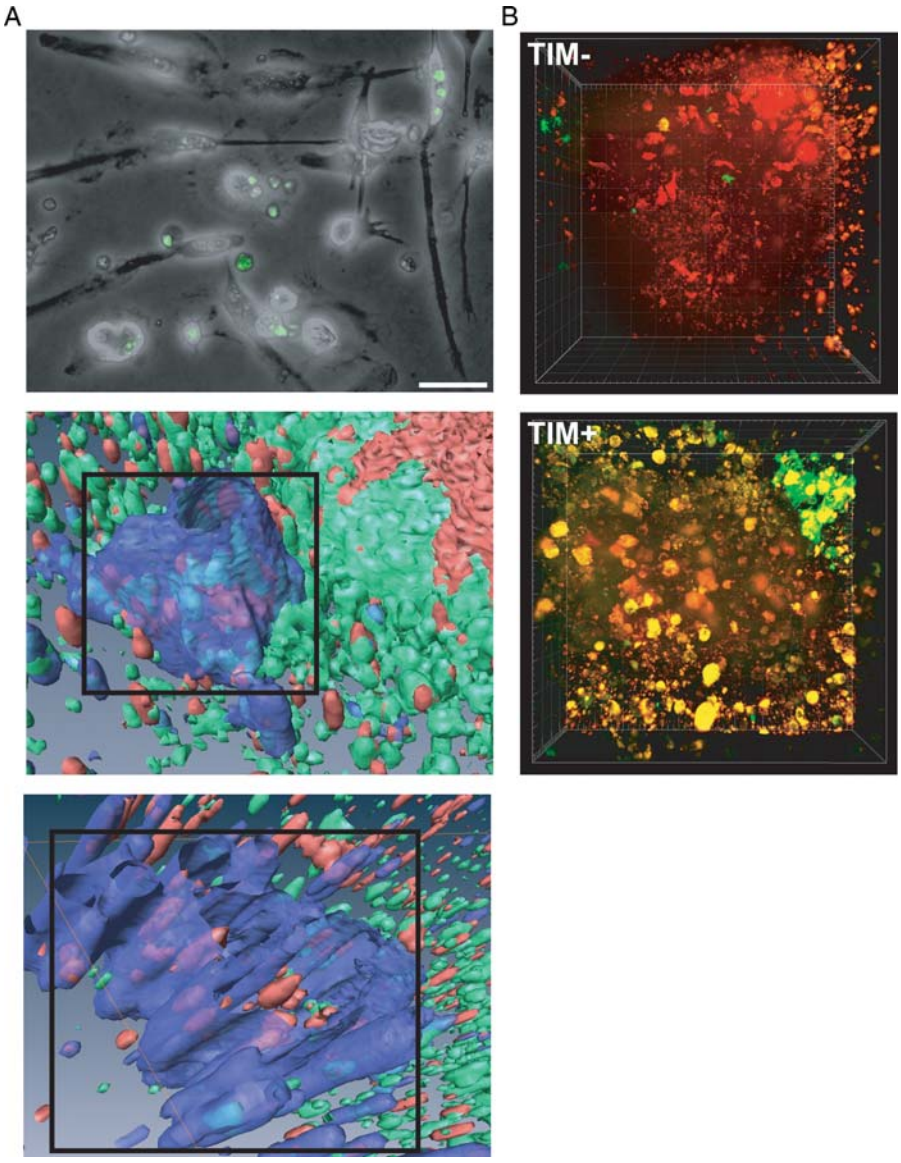

Fig. 8. TIMs pre-treated with poly (I:C) phagocytose dying/dead tumor cells. (A) Top: TIM monolayers pre-treated 48 h with poly (I:C) phagocytose CFSE labeled-NCH82 cells (green fluorescence) upon co-culture for 4 days (cell preparations shown in Fig. 7A). Bar = 50 μm. Middle and bottom images: pretreated TIMs phagocytose tumor cells in spheroid culture. Culture was performed as described in legend to Fig. 7B–C. Modeling of confocal images with the Amira software (3D iso-surface rendering view) identifies dying or dead (red label) tumor cells (green label) that are present inside TIMs (blue label) (framed areas). Data from one representative TIM preparation ($n = 3$). (B) Analysis of TIMs-tumor spheroid coculture (performed as described in legend to Fig. 7B–C) by 2-photon microscopy. Top and middle images: tumor cells, red label; TIMs, green label; sites of tumor cells engulfment by TIMs, yellow label. Data from one representative TIM preparation ($n = 2$).

Discussion

Human Microglia/Macrophages Isolated From Brain Tumor Tissues Support Tumor Growth and Invasion

Because of an improved isolation protocol, we could purify microglia/macrophages from tumor tissues in numbers high enough to perform various analyses of the same preparation. Regardless of the grade of the tumor that they originated from, these preparations appeared to be very homogenous, as indicated by transcriptional analysis and by the reproducibility in the phenotypical and functional profile of untreated and of poly (I:C)–treated TIMs. In view of the reported heterogeneity of tumor-infiltrating macrophages,[19] we can only speculate on the cause of this homogeneity (in vitro culture conditions or grade-independent tumoral factors). It is, however, remarkable that untreated TIMs in vitro exhibited a skewed M2 phenotype, as described for tumor-associated-macrophages[4] and glioma-

associated microglia/macrophages,[20] and tumor-supportive features as observed in vivo. Similar to their murine counterparts,[14,21,22] human TIMs supported proliferation, migration, and invasion of glioma cells via soluble factors.

Poly (I:C) Activates a Range of Antitumor Activities in TIMs

Human microglia isolated from healthy brain are highly reactive to poly (I:C) and respond by secreting cytokines like TNF-α and IL-6.[7] We show here, for the first time to our knowledge, that exogenously added poly (I:C) and no other TLR agonist triggered TIMs to mount a strong antitumor response mediated by soluble factors. This antitumor response appears to be particularly efficient because it is observed both toward glioma cell monolayers and toward spheroids, which exhibit a higher resistance to chemotherapeutic drugs than do monolayers.[23] TIM factors impaired tumor proliferation, migration, and invasion, and they induced cell death. In agreement with this antitumor response, transcriptome analysis showed polarization toward an M1-like profile after poly (I:C) treatment.[4] We are currently mining the TIM transcriptome in search of the cytotoxic factors. TNF-α and IFN-α, 2 prominent cytokines released after TLR3 stimulation, have been reported to be tumoricidal.[24] Single doses or combination of these cytokines did not kill the glioma cell lines (data not shown). On the basis of our observations in the mouse model,[14] we suspect that various TIM factors are responsible for this cytotoxicity.

Glioma cell lines responded with different sensitivities to both supernatants of untreated and TIM cytotoxicity. This variability, which does not depend on TIM preparations but on the glioma cell line used, most likely reflects the individual nature of the tumor tissues from which they derived and, possibly, the heterogenous nature of the tumor mass. This variability and the accompanying resistance to chemotherapeutic drugs represents a main obstacle to efficient therapies. It is therefore remarkable that tumor cells showing resistance to TIM cytotoxicity were arrested in their growth or migration abilities by these poly (I:C)–treated TIMs, as was the glioma stem cell line that we tested, despite the known resistance of these cells to cytotoxic treatments.[10]

Similar to mouse LPS/IFN-γ-treated microglia,[14] human poly (I:C)–treated microglia secreted factors that did not affect the viability of human astrocytes or neurons. The conditioned medium of human inflammatory macrophages has been reported to kill tumor cells without affecting nontransformed cells.[5] In our model, specificity of action likely results from an appropriate combination of TIM-secreted neuro/tumoricidal (eg, TNF-α) and neurotrophic factors[25] that trigger tumor cell death and support survival of nontransformed brain cells. TIMs therefore can be properly activated to exert a range of antitumor activities that preserve nontransformed cells. It will be very interesting to uncover the molecular signature of such an M1-like, neuroprotective cell.

Poly (I:C) Fails to Stimulate TIM Cytotoxicity in Presence of Glioma Cells

Observations that poly (I:C) induces direct tumor cell death in vitro[26] raised hope for its therapeutic use. However, experiments in the mouse model demonstrated a low efficiency of poly (I:C).[27] Treatment of anaplastic glioma patients did not improve the 6 months progression-free survival.[28] Some of our observations may provide an explanation to the limited success of these studies. Indeed, direct application of poly (I:C) to mixed tumor-TIM spheroids did not lead to tumor cell death for at least 2 reasons: inhibition by glioma cell supernatants of poly (I:C) activation of TIMs and increased release of anti-inflammatory factors by poly (I:C) treated glioma cells. A similar inhibition of TLR-mediated activation of microglia by GBM cells was reported by Kostianovsky et al.[29] Together, these results suggest that direct application of poly (I:C) to the tumor mass is counter-productive, because it enhances a protumor environment.

Poly (I:C)–Preactivated TIMs Suppress Tumor Growth in Coculture Systems

Strategies based on ex vivo cell activation may help to circumvent the glioma cell-mediated suppression of TIM's poly (I:C) activation. Protocols used in clinical trials and based on ex vivo activation of T cells[30] or macrophages[31] have shown few adverse effects and promising clinical results. The success of this strategy relies partly on the capacity of ex vivo activated cells to remain viable and activated after stimulus withdrawal. This was the case for poly (I:C)–stimulated TIMs. These cells infiltrated glioma cell spheroids in higher number than did nonstimulated TIMs. Prestimulated TIMs could kill and phagocytose tumor cells to a high extent over the 2-week incubation period. We hypothesize that tumor cells killed by TIMs at an early time point further activated them, thereby leading to sustained microglial activation. This activation may be mediated by danger-associated molecular patterns (DAMP) that are released by apoptotic cells and that would interact with TLRs or other pattern recognition receptors[32] expressed by TIMs. Among these DAMP, purinergic molecules, such as ATP, that are known to attract microglia[33] and mediate their activation,[34] heat shock proteins, or HMGB1,[35] are highly relevant candidates that may play a critical role in keeping TIMs activated.

The capacity of TIMs to engulf dying/dead glioma cells suggests that TIMs might eventually function as antigen presenting cells. Jack et al. showed that poly (I:C)–activated microglia derived from healthy brain tissue can mediate Th_1 polarization of T helper cells, thereby possibly facilitating cellular adaptive immune responses.[8] In this context, it is worth mentioning that

oncolytic viruses, such as Newcastle disease virus (NDV), which generates double stranded RNA species (the natural TLR3 ligands), have been used in clinical trials. Steiner et al. reported that autologous glioma cells derived from patients with GBM, infected ex vivo with NDV, irradiated, and injected back to the patient led to significant increases in progression-free and overall survival.[36] The high infiltration of tumor tissue by CD8 T cells they observed suggests a successful activation of innate immune cells that mediated an adaptive immune response.

Our study demonstrates that poly (I:C) is a potent activator of human tumor-infiltrating microglia/macrophages and can divert these highly plastic cells from the tumor influence to trigger their antitumor activities. Ex vivo activation of TIMs with this TLR3 ligand appears therefore as a very attractive and promising approach. Its combination to current therapeutic strategies might improve treatment efficiency and, thus, deserves further investigation.

Supplementary Material

Supplementary material is available online at Neuro-Oncology (http://neuro-oncology.oxfordjournals.org/).

Acknowledgments

We thank Prof. Rommelaere for his continuous support. We acknowledge support by the Deutsches Krebsforschungszentrum PhD Program (T. Kees, J. Noack), the Deutscher Akademischer Austausch Dienst PhD Program (R. Mora), and the Centre National de la Recherche Scientifique (A. Régnier-Vigouroux). Support by the Deutsches Krebsforschungszentrum Light Microscopy Facility is gratefully acknowledged.

Conflict of interest statement. None declared.

Funding

This work was supported by Tumorzentrum Heidelberg-Mannheim (to C.H.-M.); Deutsche Krebshilfe (#109202 to C.H.-M.); HGF Alliance Immunotherapy-Immunomonitoring (to C.S.F.), German Federal Ministry of Education and Research (BMBF) within the National Genome Research Network NGFNplus (#01GS0883 to B.R.).

References

1. Giometto B, Bozza F, Faresin F, Alessio L, Mingrino S, Tavolato B. Immune infiltrates and cytokines in gliomas. *Acta Neurochir (Wien)*. 1996;138(1):50–56.
2. Kreutzberg GW. Microglia: a sensor for pathological events in the CNS. *Trends in Neurosciences*. 1996;19(8):312–318.
3. Watters JJ, Schartner JM, Badie B. Microglia function in brain tumors. *J Neurosci Res*. 2005;81(3):447–455.
4. Mantovani A, Sica A, Allavena P, Garlanda C, Locati M. Tumor-associated macrophages and the related myeloid-derived suppressor cells as a paradigm of the diversity of macrophage activation. *Human Immunology*. 2009;70(5):325–330.
5. Turyna B, Jurek A, Gotfryd K, Siaskiewicz A, Kubit P, Klein A. Peritonitis-induced antitumor activity of peritoneal macrophages from uremic patients. *Folia Histochem Cytobiol*. 2004;42(3):147–153.
6. Chen K, Huang J, Gong W, Iribarren P, Dunlop NM, Wang JM. Toll-like receptors in inflammation, infection and cancer. *International Immunopharmacology*. 2007;7(10):1271–1285.
7. Jack CS, Arbour N, Manusow J, et al. TLR signaling tailors innate immune responses in human microglia and astrocytes. *J Immunol*. 2005;175(7):4320–4330.
8. Jack CS, Arbour N, Blain M, Meier UC, Prat A, Antel JP. Th1 polarization of CD4+ T cells by Toll-like receptor 3-activated human microglia. *J Neuropathol Exp Neurol*. 2007;66(9):848–859.
9. Hussain SF, Yang D, Suki D, Grimm E, Heimberger AB. Innate immune functions of microglia isolated from human glioma patients. *J Transl Med*. 2006;4:15.
10. Campos B, Wan F, Farhadi M, et al. Differentiation Therapy Exerts Antitumor Effects on Stem-like Glioma Cells. *Clin Cancer Res*. 2010;16(10):2715–2728.
11. Karcher S, Steiner HH, Ahmadi R, et al. Different angiogenic phenotypes in primary and secondary glioblastomas. *Int J Cancer*. 2006;118(9):2182–2189.
12. Burudi EM, Riese S, Stahl PD, Regnier-Vigouroux A. Identification and functional characterization of the mannose receptor in astrocytes. *Glia*. 1999;25(1):44–55.
13. Herold-Mende C, Seiter S, Born AI, et al. Expression of CD44 splice variants in squamous epithelia and squamous cell carcinomas of the head and neck. *The Journal of Pathology*. 1996;179(1):66–73.
14. Mora R, Abschuetz A, Kees T, et al. TNF-alpha- and TRAIL-resistant glioma cells undergo autophagy-dependent cell death induced by activated microglia. *Glia*. 2009;57(5):561–581.
15. Xu L, Deng X. Protein kinase Ciota promotes nicotine-induced migration and invasion of cancer cells via phosphorylation of micro- and m-calpains. *J Biol Chem*. 2006;281(7):4457–4466.
16. Nickles D, Abschuetz A, Zimmer H, et al. End-stage dying glioma cells are engulfed by mouse microglia with a strain-dependent efficacy. *J Neuroimmunol*. 2008;197(1):10–20.
17. Parney IF, Waldron JS, Parsa AT. Flow cytometry and in vitro analysis of human glioma-associated macrophages. Laboratory investigation. *J Neurosurg*. 2009;110(3):572–582.
18. Seglen PO, Gordon PB. 3-Methyladenine: specific inhibitor of autophagic/lysosomal protein degradation in isolated rat hepatocytes. *Proceedings of the National Academy of Sciences of the United States of America*. 1982;79(6):1889–1892.
19. Movahedi K, Laoui D, Gysemans C, et al. Different tumor microenvironments contain functionally distinct subsets of macrophages derived from Ly6C(high) monocytes. *Cancer Research*. 2010;70(14):5728–5739.

20. Komohara Y, Ohnishi K, Kuratsu J, Takeya M. Possible involvement of the M2 anti-inflammatory macrophage phenotype in growth of human gliomas. *The Journal of Pathology*. 2008;216(1):15–24.
21. Markovic DS, Glass R, Synowitz M, Rooijen N, Kettenmann H. Microglia stimulate the invasiveness of glioma cells by increasing the activity of metalloprotease-2. *J Neuropathol Exp Neurol*. 2005;64(9): 754–762.
22. Sliwa M, Markovic D, Gabrusiewicz K, et al. The invasion promoting effect of microglia on glioblastoma cells is inhibited by cyclosporin A. *Brain*. 2007;130(Pt 2):476–489.
23. Hamilton G. Multicellular spheroids as an in vitro tumor model. *Cancer Lett*. 1998;131(1):29–34.
24. Remels L, Fransen L, Huygen K, De Baetselier P. Poly I:C activated macrophages are tumoricidal for TNF-alpha-resistant 3LL tumor cells. *J Immunol*. 1990;144(11):4477–4486.
25. Kim SU, de Vellis J. Microglia in health and disease. *J Neurosci Res*. 2005;81(3):302–313.
26. Paone A, Starace D, Galli R, et al. Toll-like receptor 3 triggers apoptosis of human prostate cancer cells through a PKC-alpha-dependent mechanism. *Carcinogenesis*. 2008;29(7):1334–1342.
27. Grauer OM, Wesseling P, Adema GJ. Immunotherapy of diffuse gliomas: biological background, current status and future developments. *Brain Pathol*. 2009;19(4):674–693.
28. Butowski N, Lamborn KR, Lee BL, et al. A North American brain tumor consortium phase II study of poly-ICLC for adult patients with recurrent anaplastic gliomas. *J Neurooncol*. 2009;91(2):183–189.
29. Kostianovsky AM, Maier LM, Anderson RC, Bruce JN, Anderson DE. Astrocytic regulation of human monocytic/microglial activation. *J Immunol*. 2008;181(8):5425–5432.
30. Plautz GE, Miller DW, Barnett GH, et al. T cell adoptive immunotherapy of newly diagnosed gliomas. *Clin Cancer Res*. 2000;6(6):2209–2218.
31. Sutton L, Chaoui D, Cazin B, et al. Autologous activated macrophages (MAK) coated ex vivo with humanized anti-CD20 monoclonal antibodies can eradicate minimal residual disease in chronic lymphocytic leukaemia in clinical response. *Br J Haematol*. 2008;142(6):996–998.
32. Zitvogel L, Kepp O, Kroemer G. Decoding cell death signals in inflammation and immunity. *Cell*. 2010;140(6):798–804.
33. Gyoneva S, Orr AG, Traynelis SF. Differential regulation of microglial motility by ATP/ADP and adenosine. *Parkinsonism Relat Disord*. 2009;15(Suppl 3):S195–S199.
34. Skaper SD, Debetto P, Giusti P. The P2X7 purinergic receptor: from physiology to neurological disorders. *FASEB J*. 2010;24(2):337–345.
35. Hoarau JJ, Krejbich-Trotot P, Jaffar-Bandjee MC, et al. Activation and control of CNS innate immune responses in health and diseases: a balancing act finely tuned by neuroimmune regulators (NIReg). *CNS & Neurological Disorders Drug Targets*. 2011;10(1):25–43.
36. Steiner HH, Bonsanto MM, Beckhove P, et al. Antitumor vaccination of patients with glioblastoma multiforme: a pilot study to assess feasibility, safety, and clinical benefit. *J Clin Oncol*. 2004;22(21):4272–4281.